

# Upwelling Intensification As Part of the Pliocene-Pleistocene Climate Transition

Jeremy R. Marlow,<sup>1\*</sup> Carina B. Lange,<sup>2</sup> Gerold Wefer,<sup>3</sup>  
Antoni Rosell-Melé<sup>4</sup>

A deep-sea sediment core underlying the Benguela upwelling system off southwest Africa provides a continuous time series of sea surface temperature (SST) for the past 4.5 million years. Our results indicate that temperatures in the region have declined by about 10°C since 3.2 million years ago. Records of paleoproductivity suggest that this cooling was associated with an increase in wind-driven upwelling tied to a shift from relatively stable global warmth during the mid-Pliocene to the high-amplitude glacial-interglacial cycles of the late Quaternary. These observations imply that Atlantic Ocean surface water circulation was radically different during the mid-Pliocene.

Earth's climate system has developed from a state of relative global warmth during the mid-Pliocene [ $\sim 3.2$  to 4.5 million years ago (Ma)], with ice sheets restricted to the Antarctic, to a globally cooler state during the late Pleistocene, with extensive bipolar ice sheets and increased pole-equator temperature gradients (1, 2). The cooling transition was accentuated by a combination of external forcings that included tectonic modifications to the atmosphere-ocean circulation system (3), fluctuations in solar insolation from variations in Earth's orbit (2), and variable global geologic weathering rates (4). The transition probably began with the closure of the Central American Seaway (CAS) during the late Pliocene that promoted the production of North Atlantic Deep Water (NADW) (3, 5), which allowed for the piracy of surface water heat from the South Atlantic to the North Atlantic. The initial Northern Hemisphere warming induced by CAS closure could be considered a temporary "detour" in an ongoing ( $\sim 40$  million years long) cooling trend (6–8) that resumed when Northern Hemisphere glaciation (NHG) intensified (3.1 to 2.5 Ma) in response to an increase in the amplitude of Earth's orbital obliquity during this critical period (3). At  $\sim 0.9$  Ma, the cooling appears to have moved the global climate system into a mode of high-amplitude, bipolar, glacial-interglacial (G-IG) cycles

lasting throughout the late Pleistocene (9).

Quantitative temperature reconstructions for the Pliocene-Pleistocene cooling transition are needed to understand the processes that have caused Earth's climate to enter the G-IG quasi-stable state (10, 11) but have thus far been limited by shortcomings in the proxy techniques used (12, 13). Here we report estimates of past sea surface temperatures (SSTs) using the  $U_{37}^{K'}$  index (14, 15) for the Pliocene-Pleistocene, measured in marine sediments recovered from Ocean Drilling Program (ODP) Site 1084 (25°31'S, 13°2'E; North Cape Basin; water depth, 1992 m). In addition, we report estimates of paleoproductivity from the mass accumulation rates of organic carbon (MAR  $C_{org}$ ), diatom abundances, and diatom assemblages.

Site 1084 is situated off the coast of Namibia (Fig. 1) and provides a well-preserved and continuous sedimentary record of the Benguela Current (BC) upwelling system from the mid-Pliocene (4.6 Ma) to the late Pleistocene (0.1 Ma). South Atlantic Central Water (SACW) is upwelled into the BC from a depth of about 200 m, forming filaments of cold nutrient-rich waters that extend well offshore and mix with low-productivity oceanic water, forming a zone of year-round high phytoplankton productivity (16). The BC is the eastern boundary current of the South Atlantic gyre and is analogous to the currents off California, Peru, and northwest Africa, but with a more restricted field of cool SST and larger amounts of surface nutrients (17). The BC upwelling system augments the regulation of the atmosphere-ocean carbon cycle through biological pumping and dumping of  $CO_2$  (6) and modulates the climate of southern Africa by restricting the amount of evaporation for onshore precipitation. Previous long-term reconstructions suggest that the BC responded to the Plio-

cene-Pleistocene cooling transition with increased upwelling of nutrient-rich waters (18–20) and by forcing climatically mediated events on the southern African continent (18). The high sedimentation rates [10 to 27 cm per thousand years (ky)] and organic carbon contents (2 to 18%) provide excellent conditions favorable for  $U_{37}^{K'}$  analysis. In contrast, these conditions make reconstructions using planktonic foraminifera difficult and possibly unreliable, owing to severe carbonate dissolution (21).

Our SST record for Site 1084 (Fig. 2B, red curve) shows a decline of  $\sim 10^\circ C$  since 3.2 Ma. We believe that this large cooling signal was caused by a combination of global long-term cooling and regional changes in surface water conditions from increased upwelling. Increases in MAR  $C_{org}$  (Fig. 2C), diatom abundance (Fig. 2D), and the proportion of upwelling species in the diatom assemblage (Fig. 2E) are synchronous with the general cooling. This inverse relationship between paleoproductivity and SST is evidence that there was a trend toward increased upwelling of cool nutrient-rich waters, which consequently would have enhanced the global cooling signal. The global component of the paleo-SST record is reflected in the similarity of its profile with the profile of the established global ice volume record (Fig. 2A), taken from (2) and (22).

We have subdivided all the records into five phases to aid interpretation. Phase I (4.6 to 3.2 Ma, mid-Pliocene) is characterized by warm SSTs with three cool excursions ( $1^\circ$  to  $2^\circ C$  at 4.1, 3.7, and 3.2 Ma) that are probably related to increased Antarctic glaciation (2). The sharp cooling at 3.2 Ma marks the onset of a prolonged gradual cooling (Phase II, 3.2 to 2.1 Ma, late Pliocene) concomitant with the initiation of NHG (3), with major cooling excursions ( $2^\circ C$  at 2.8 and 2.5 Ma) equivalent to events in the ice volume records. The transition from Phase II to III is marked by a rapid decline in SST ( $2^\circ$  to  $3^\circ C$  at 2.1 to 1.9 Ma) that is coincident with the onset of more intense glacials. Phase III (2.0 to 1.4 Ma) highlights an apparent pause in the cooling trend but with increasing variability that possibly reflects the increased amplitude in the ice volume record at 41-ky obliquity frequencies (22), although the average sampling interval in the SST record ( $\sim 50$  ky) does not allow a detailed orbital scale interpretation. Phase IV includes a SST "crash" that is coincident with further intensification of global ice volume during glacials, followed by a transition at 0.6 Ma to fluctuating SSTs similar to the  $\sim 100$ -ky G-IG cyclicity (Phase V) and with an amplitude ( $5^\circ$  to  $7^\circ C$ ) comparable to other late Quaternary  $U_{37}^{K'}$  reconstructions for the BC (23).

The average SST for the mid-Pliocene

<sup>1</sup>Department of Fossil Fuels and Environmental Geochemistry, Drummond Building, University of Newcastle, Newcastle upon Tyne, NE1 7RU, UK. <sup>2</sup>Geosciences Research Division, Scripps Institution of Oceanography, University of California at San Diego, La Jolla, CA 92093, USA. <sup>3</sup>Department of Earth Sciences (FB-5), University of Bremen, Postfach 330440, 28334 Bremen, Germany. <sup>4</sup>Department of Geography, University of Durham, Durham, DH1 3LE, UK.

\*To whom correspondence should be addressed. E-mail: J.R.Marlow@ncl.ac.uk

(Phase I) is 26°C, which is approximately 8°C warmer than the annual average SST of the modern overlying waters (17) and the preceding four interglacials (tentatively labeled after marine isotope stages 5, 7, 9, and 11 in Fig. 2B). A combination of previously reported  $U_{37}^K$  reconstructions for the eastern boundary (Canary Current, ODP Site 958) of the North Atlantic (Fig. 2B, blue curve) also reveals a significant SST decline (~5°C) between the mid-Pliocene (24) and late Quaternary interglacials (25). Time-slice SST reconstructions based on planktonic assemblages from sediments located away from the main upwelling cells (Walvis Ridge) estimated the mid-Pliocene-to-modern SST decline to be 2°C (12, 18). These reconstructions are difficult to interpret quantitatively because species extinctions during the late Pliocene and Pleistocene mean that contiguous modern analogous assemblages do not exist (23). The work presented here and results from chemotaxonomic (23, 26–28) and early/pre-Quaternary (24, 29) studies suggest that  $U_{37}^K$  does not appear to be significantly affected by either Pliocene-Pleistocene species extinctions or variations in production depth, nutrients, and seasonal production maxima. The global calibration used in this study (28) probably remains applicable throughout the Pliocene-Pleistocene and the standard error of the calibrated SST estimate ( $\pm 1.0^\circ\text{C}$ ) is within the temperature ranges reported here. The suboxic sediments at Site 1084 are not typical for conditions where postdepositional alkenone diagenesis may be significant (30, 31). Moreover, complete diagenetic removal of the more unsaturated alkenone has not occurred in samples from the mid-Pliocene warm period because  $U_{37}^K < 1$  throughout.

The diatom maximum during Phase II (3.2 to 2.2 Ma) appears out of sequence with the other two paleoproductivity records. The species composition of the diatom maximum points to subsurface advection of antarctic/subantarctic diatoms and a possible increase in the abundance of the in situ planktonic assemblage (Fig. 2E), arising from a change in the quality of nutrients in the upwelled water mass (21). Advection is indicated by the presence of extensive *Thalassiothrix antarctica* mats (32) in a pulse of Southern Ocean-dwelling species (SO) without an accompanying decline in the abundance of warm species (Fig. 2E) or an increase in  $MAR C_{org}$  (a proxy for total paleoproductivity). The advected flux of diatoms and nutrients could have arrived in Antarctic Intermediate Water (AAIW), a phenomenon that has been observed in sediment traps underlying the BC (33). The *T. antarctica* mats could have formed at the frontal zone of sinking AAIW in the Subtropical Convergence Zone

(SCZ). The increased supply of NADW to the surface circum-Antarctic seas after CAS closure (20) could have provided the increased biosiliceous export required to produce the diatom maximum. In addition, the frontal systems (including the SCZ) migrated northward toward the BC as Antarctic ice volume increased (from ~3.2 Ma onward) and the sea ice boundary advanced (18, 32, 34). As NHG intensified (from 2.7 Ma onward), the supply of NADW and dissolved silicate reduced (3, 6). By 2.1 to 1.9 Ma, a threshold appears to have been reached; the SO component of the diatom assemblage was almost entirely removed (Fig. 2E) and the diatom abundance maximum was terminated. However, diatom abundances did not return to the previously low values of the mid-Pliocene but remained relatively high after the termination, albeit with increased variability. This elevated diatom abundance relative to the mid-Pliocene could be attributed to increased in situ diatom production owing to increased wind-driven upwelling of cool nutrient-rich SACW, as indicated by the enhanced abundance of upwelling species (Fig. 2E), the reduced SST (Fig. 2B, red curve), and increased  $MAR C_{org}$  (Fig. 2C).

Previous records of aeolian dust flux to

marine sediments (22, 35, 36) suggested increased trade wind strength and aridification of Africa throughout the cooling transition. This increase in atmospheric circulation would have been driven by a steeper pole-equator temperature gradient owing to the development of the bipolar cryosphere (during Phase II). We hypothesize that the intensification of trade winds initiated a positive feedback cycle, whereby increased trade wind-driven upwelling enhanced the long-term (>100 ky) “leak” of  $\text{CO}_2$  from the global ocean-atmosphere system as sedimentary organic carbon. A consequent reduction in greenhouse forcing could have contributed to further cooling and bipolar ice sheet expansion, leading to further amplification of the pole-equator temperature gradient. The increase in aridity would have increased the supply of nutrients to the oceans that would have been necessary to sustain an increase in the biologically driven ocean carbon pump. A mechanism of this type working on time scales of >100 ky may have been an important component of changes in the global carbon cycle and may have been partly responsible for allowing the climatic transition to proceed (4, 10, 37–39). Our results for the BC upwelling system suggest that the mechanism

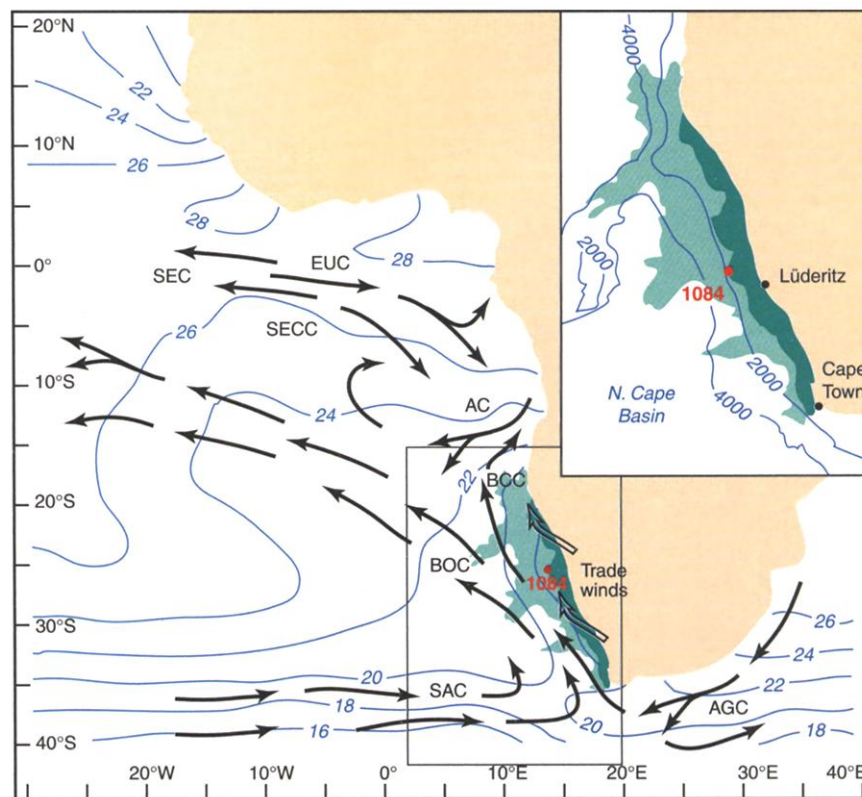


**Fig. 1.** Map of Site 1084 locality and modern oceanographic setting. The inset illustrates the areal extent of year-round (dark shading) and filamentous (light shading) BC upwelling for August 1984 (16). Isotherms reflect annual average SSTs (17). Open arrows show the trajectories of trade winds over southwest Africa. Solid arrows indicate dominant surface and near-surface ocean currents: AC, Angola Current; AGC, Agulhas Current; BCC, Benguela Coastal Current; BOC, Benguela Oceanic Current; EUC, Equatorial Undercurrent; SAC, South Atlantic Current; SEC, South Equatorial Current; and SECC, South Equatorial Countercurrent.

REPORTS

became pronounced at 2.1 to 1.9 Ma and intensified during the period leading to the onset of the 100-ky G-IG cycles at ~0.6 Ma.

The intensification of BC upwelling would have had a direct regional influence by affecting the climate of southern Africa. A reduction in onshore precipitation owing to

cooler coastal surface waters would have compounded the shift from mesic to xeric conditions observed in this region during the Pliocene-Pleistocene (18, 40), a transition that may have forced local speciation events (40, 41). For example, the emerging occurrence of the *Homo* genus at ~2 Ma in the

region coincided with a large increase in mammals adapted to grazing and arid conditions (41). Both events appear to be synchronous with the abrupt cooling and productivity increase of the BC at 2.1 to 1.9 Ma.

The equatorward surface Benguela Ocean Current (BOC) would have been present dur-

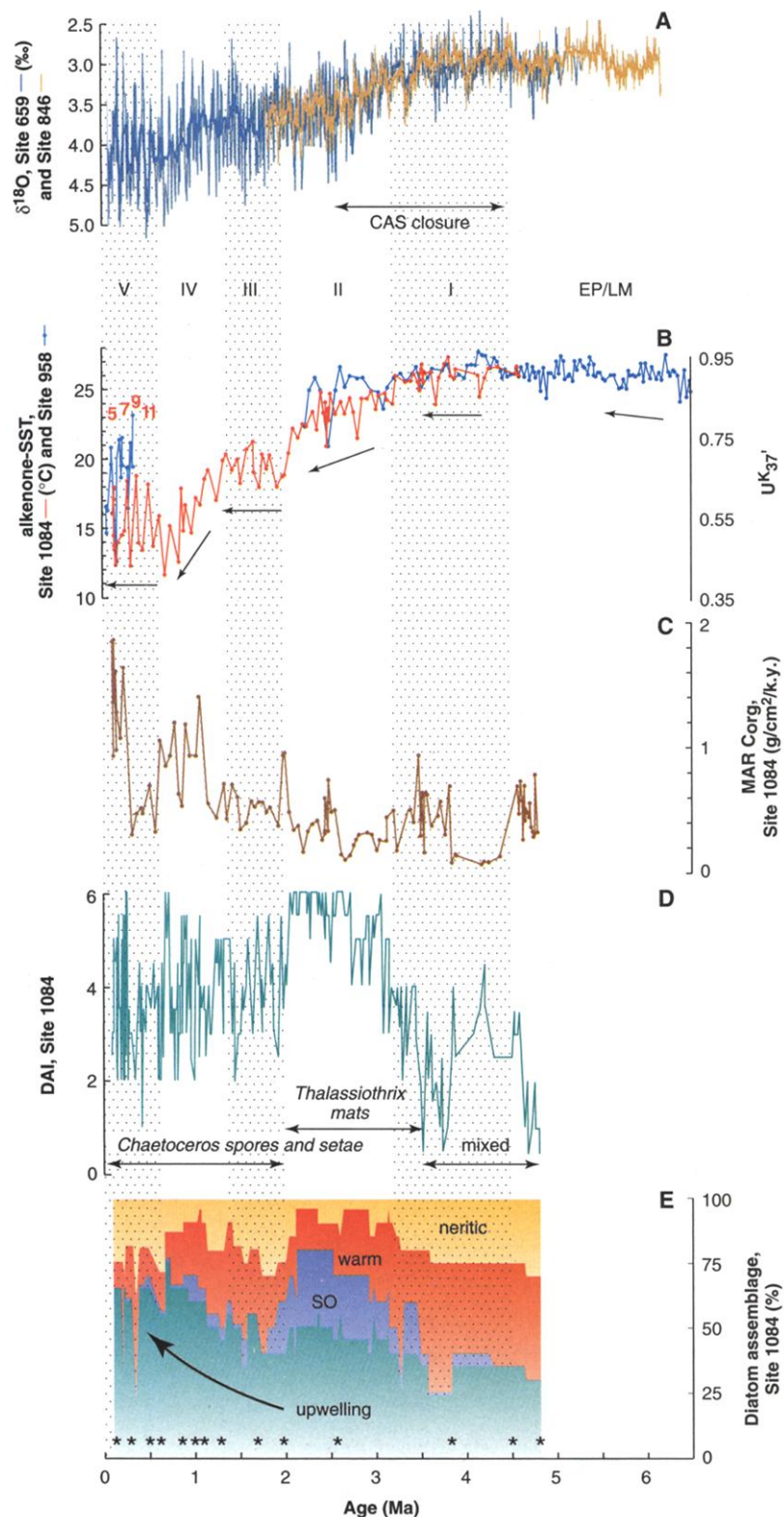


**Fig. 2.** Results from ODP Site 1084 compared to benthic foraminiferal oxygen isotope ( $\delta^{18}\text{O}$ ) records (a proxy for global ice volume). (A) Benthic  $\delta^{18}\text{O}$  curve from Sites 659 (blue) (22) and 846 (orange) (2). Thin lines are original data and thick lines are smoothed data with a 20-point running mean. In (A) through (E), the records have been divided into five discrete phases (I through V) to aid interpretation. EP, early Pliocene; LM, late Miocene; CAS, Central American Seaway. (B) SST record from Site 1084 (red) derived from  $U_{37}^K$  values using global core-top calibration (28). Alkenones were measured according to the methods of Rosell-Melé (42) and were  $>10 \mu\text{g/g}$  of dry sediment throughout the core (analytical precision =  $\pm 1.0^\circ\text{C}$ ).  $U_{37}^K$ -based SST data from Site 958 are superimposed (blue) (24, 25). Numbers refer to marine oxygen isotope stages. (C) Site 1084 MAR  $C_{org}$ , calculated as in Emeis *et al.* (29) from dry bulk densities and linear sedimentation rates. (D) Site 1084 diatom abundance index as reported in Lange *et al.* (32). Horizontal arrows denote dominant diatom assemblages for the Pleistocene (*Chaetoceros*), late Pliocene (*Thalassiothrix*), and mid-Pliocene (mixed). (E) Site 1084 relative diatom assemblage (this study) (43). Asterisks indicate datums from the shipboard biostratigraphic and magnetic polarity reversal age model (44). Although the age model is not as precisely dated as orbitally tuned records, it is sufficient for the long-term and low-resolution study reported here. Temporal resolution is  $<50$  ky throughout the majority of the core, with high-resolution intervals ( $\sim 5$  ky) at 0.09 to 0.13 Ma, 2.43 to 2.48 Ma, and 3.47 to 3.53 Ma.

ing the mid-Pliocene to feed the enhanced production of NADW (3, 5, 6, 38). However, our results suggest that the manifestation of the BOC as a characteristic intrusion of cold surface water across the modern South Atlantic (Fig. 1) would have been less pronounced during the mid-Pliocene, because the BC would have upwelled less of the cool SACW. Our mid-Pliocene SST estimates for the BC upwelling system (~26°C) are similar to the average annual SST for the modern oligotrophic waters of the western South Atlantic (~25°C) at the same latitude (Fig. 1). However, global mid-Pliocene warmth would have had a basinwide influence, so that the SST for the western boundary would probably have remained higher than for the eastern boundary (12), because our paleoproductivity records and previous studies indicate that a degree of upwelling continued throughout the mid-Pliocene (18–20).

The processes related to enhanced BC upwelling discussed here may have occurred at the eastern boundaries of the other three major Atlantic and Pacific Ocean basins. These systems could have provided additional long-term sinks for atmospheric CO<sub>2</sub> through the hypothetical mechanism outlined above. The cooling of the Canary Current (24, 25) suggests that the process may have occurred at the North Atlantic's eastern boundary. The development of the U<sub>37</sub><sup>K</sup> technique for quantitative late Neogene SST reconstruction in sediment cores from a variety of oceanographic settings should allow these and other hypotheses about changes in global and regional paleotemperatures over the past 5 million years to be tested further.

References and Notes

1. D. A. Hodell, K. Venz, in *Antarctic Research Series*, J. P. Kennett, D. A. Warnke, Eds. (American Geophysical Union, Washington, DC, 1992), vol. 56, pp. 265–310.
2. N. J. Shackleton, M. A. Hall, D. Pate, *Proc. ODP Sci. Res.* **138**, 337 (1995).
3. G. H. Haug, R. Tiedemann, *Nature* **393**, 673 (1998).
4. C. France-Lanord, L. A. Derry, *Nature* **390**, 65 (1997).
5. K. Billups, A. C. Ravelo, J. C. Zachos, *Paleoceanography* **13**, 84 (1998).
6. W. H. Berger, G. Wefer, in *The South Atlantic: Present and Past Circulation*, G. Wefer, W. H. Berger, G. Siedler, D. J. Webb, Eds. (Springer, Heidelberg, Germany, 1996), pp. 363–410.
7. K. G. Miller, R. G. Fairbanks, G. S. Mountain, *Paleoceanography* **2**, 1 (1987).
8. J. A. Barron, J. G. Baldauf, in *Productivity of the Ocean: Present and Past*, W. H. Berger, V. S. Smetacek, G. Wefer, Eds. (Wiley, New York, 1989), pp. 341–354.
9. W. F. Ruddiman, *Paleoceanography* **4**, 353 (1989).
10. D. Rind, *J. Geophys. Res.* **103**, 5943 (1998).
11. L. C. Sloan, T. J. Crowley, D. Pollard, *Mar. Micropaleontol.* **27**, 51 (1996).
12. H. J. Dowsett, J. Barron, R. Poore, *Mar. Micropaleontol.* **27**, 13 (1996).
13. H. J. Dowsett, R. Z. Poore, *Mar. Micropaleontol.* **16**, 1 (1990).
14. The U<sub>37</sub><sup>K</sup> index is based on the ratio of di- and tri-unsaturated *n*-C<sub>37</sub> alkenones produced by specific species of haptophyte algae.
15. S. C. Brassell, G. Eglinton, U. Pflaumann, M. Sarnthein, *Nature* **320**, 129 (1986).
16. J. R. E. Lutjeharms, P. L. Stockton, *S. Afr. J. Mar. Sci.* **5**, 35 (1987).

17. S. Levitus, T. Boyer, *World Ocean Atlas 1994. Vol. 4. Temperature* (U.S. Department of Commerce, Washington, DC, 1994).
18. L. Diester-Haass, P. A. Meyers, P. Rothe, in *Upwelling Systems: Evolution since the Early Miocene*, C. P. Summerhayes, W. L. Prell, K. C. Emeis, Eds. (Geological Society Special Publication No. 63, London, 1992), pp. 331–342.
19. H. Dowsett, D. Willard, *Mar. Micropaleontol.* **27**, 181 (1996).
20. W. W. Hay, J. C. Brock, in *Upwelling Systems: Evolution since the Early Miocene*, C. P. Summerhayes, W. L. Prell, K. C. Emeis, Eds. (Geological Society Special Publication No. 63, London, 1992), pp. 463–497.
21. W. H. Berger *et al.*, *Proc. ODP Init. Rep.* **175**, 505 (1998).
22. R. Tiedemann, M. Sarnthein, N. J. Shackleton, *Paleoceanography* **9**, 619 (1994).
23. P. J. Müller, M. Cepek, G. Ruhland, R. R. Schneider, *Palaeoogeogr. Palaeoecimatol. Palaeoecol.* **135**, 71 (1997).
24. T. D. Herbert, J. D. Schuffert, *Proc. ODP Sci. Res.* **159T**, 17 (1998).
25. U. Pflaumann, M. Sarnthein, K. Ficken, A. Grothmann, A. Winkler, *Proc. ODP Sci. Res.* **159T**, 3 (1998).
26. I. T. Marlowe, S. C. Brassell, G. Eglinton, J. C. Green, *Chem. Geol.* **88**, 349 (1990).
27. T. D. Herbert *et al.*, *Paleoceanography* **13**, 263 (1998).
28. P. J. Müller, G. Kirst, G. Ruhland, I. von Storch, A. Rosell-Melé, *Geochim. Cosmochim. Acta* **62**, 1757 (1998).
29. K. -C. Emeis, H. Dooze, A. Mix, D. Schulz-Bull, *Proc. ODP Sci. Res.* **138**, 605 (1995).
30. M. J. L. Hoefs, G. J. M. Versteegh, W. I. C. Rijpstra, J. W. de Leeuw, J. S. Sinninghe Damsté, *Paleoceanography* **13**, 42 (1998).
31. C. R. Gong, D. J. Hollander, *Geochim. Cosmochim. Acta* **63**, 405 (1999).
32. C. B. Lange, W. H. Berger, H. -L. Lin, G. Wefer, Shipboard Scientific Party, *Mar. Geol.* **161**, 93 (1999).
33. U. F. Treppke *et al.*, *J. Mar. Res.* **54**, 991 (1996).
34. A. Abelmann, R. Gersonde, V. Speiss, in *Geological History of the Polar Oceans: Arctic Versus Antarctic*, U. Bleil, J. Thiede, Eds. (Kluwer, Dordrecht, Netherlands, 1990), pp. 729–759.
35. W. F. Ruddiman, T. R. Janecek, *Proc. ODP Sci. Res.* **108**, 211 (1989).

36. S. A. Hovan, D. K. Rea, *Proc. ODP Sci. Res.* **121**, 219 (1991).
37. G. H. Haug, D. M. Sigman, R. Tiedemann, T. F. Pederson, M. Sarnthein, *Nature* **401**, 779 (1999).
38. M. E. Raymo, B. Grant, M. Horowitz, G. H. Rau, *Mar. Micropaleontol.* **27**, 313 (1996).
39. A. J. Watson, in *Upwelling in the Ocean: Modern Processes and Ancient Records*, C. P. Summerhayes, K.-C. Emeis, M. V. Angel, R. L. Smith, B. Zeitzschel, Eds. (Wiley, New York, 1995), pp. 321–336.
40. P. B. de Menocal, *Science* **270**, 53 (1995).
41. K. E. Reed, *J. Hum. Evol.* **32**, 289 (1997).
42. A. Rosell-Melé, thesis, University of Bristol, UK (1994).
43. Upwelling species are associated with colder upwelled waters of the high-productivity coastal band (such as *Chaetoceros* spp., mainly *C. radicans* and *C. cinctus*; and *Thalassionema nitzschioides* var. *nitzschioides*), SO indicates a Southern Ocean assemblage composed of the subantarctic diatoms *Probotoscia barboi* and *Thalassiothrix antarctica* and of the antarctic/subantarctic radiolarian *Cycladophora plicenica*; "warm" indicates a broad variety of species widely distributed in the tropical and subtropical Atlantic [such as *Alveus* (= *Nitzschia*) *marinus*, *Azpeitia nodulifera*, *A. africana*, *Fragilariopsis* (= *Pseudoeunotia*) *doliolus*, *Hemidiscus cuneiformis*, *Rhizosolenia bergonii*, *Roperia tessellata*, *Stellarima stellaris*, and *Thalassionema nitzschioides* var. *parva*]; and "neritic" indicates planktonic (*Actinocyclus* spp., *Coscinodiscus centralis*, *C. gigas*, *C. radiatus*, *Delphineis karstenii*, *Stephanopyxis* spp., and *Thalassiosira angulata*) and tycolpelagic and benthic species (such as *Actinopterychus senarius*, *A. vulgaris*, *Cocconeis* sp., *Delphineis surirella*, and *Paralia sulcata*) characteristic of nearshore waters.
44. Shipboard Scientific Party, *Proc. ODP Init. Rep.* **175**, 339 (1998).
45. We thank W. Berger, K. Emeis, P. Farrimond, and R. Schneider for discussions and the ODP for providing samples. Supported by a studentship from the UK Natural Environment Research Council to J.R.M. and by funds from Joint Oceanographic Institutions, Inc., and the U.S. Science Support Program to C.B.L., from Deutsche Forschungsgemeinschaft to G.W., and from the European Union Environment and Climate Program to A.R.-M.

4 August 2000; accepted 16 November 2000

# Millennial-Scale Dynamics of Southern Amazonian Rain Forests

Francis E. Mayle,<sup>1\*</sup> Rachel Burbridge,<sup>1</sup> Timothy J. Killeen<sup>2,3</sup>

Amazonian rain forest–savanna boundaries are highly sensitive to climatic change and may also play an important role in rain forest speciation. However, their dynamics over millennial time scales are poorly understood. Here, we present late Quaternary pollen records from the southern margin of Amazonia, which show that the humid evergreen rain forests of eastern Bolivia have been expanding southward over the past 3000 years and that their present-day limit represents the southernmost extent of Amazonian rain forest over at least the past 50,000 years. This rain forest expansion is attributed to increased seasonal latitudinal migration of the Intertropical Convergence Zone, which can in turn be explained by Milankovitch astronomic forcing.

Understanding the long-term dynamics of Amazonian rain forest–savanna boundaries over millennial time scales can provide important insights into Amazonian paleoclimates and may also improve understanding

of rain forest biodiversity (1). However, the late Quaternary history of forest–savanna dynamics of southern Amazonia is poorly understood, based predominantly on controversial pollen data from two sites. One